Structure Mapping of 5′-^{32}P-Labeled RNA with S1 Nuclease†

Regina M. Wurst, John N. Vournakis,* and Allan M. Maxam‡

ABSTRACT: A rapid, general method for mapping RNA structure in solution using structure-specific enzymes is described. The technique is demonstrated using two transfer RNAs, yeast tRNA^{Phe} and *E. coli* tRNA$^{Glu}_2$. The 5′-terminal phosphate of the RNA is first removed with alkaline phosphatase and then replaced with [^{32}P]phosphate using T4 polynucleotide kinase and [γ-^{32}P]ATP. Under native conditions partial digestion of end-labeled tRNAs with single-strand-specific S1 nuclease generates a mixture of 5′-end-labeled oligonucleotide fragments. Limited alkaline hydrolysis provides a complete set of oligonucleotides due to cleavage at every phosphodiester bond. Partial digestions with RNases T1, U2, A, and Phy I under denaturing conditions produce end-labeled fragments having lengths representing distances from the 5′ end to guanylate, adenylate, pyrimidine, and noncytidylate residues, respectively. Electrophoresis of partial digests in parallel on 20% polyacrylamide–7 M urea gels resolves oligonucleotides that differ in length by one nucleotide. The exact positions at which S1 nuclease cleaves these molecules are mapped by comparing the locations of S1-generated bands with bands of known lengths produced by the alkali and base-specific RNases. The anticodon loop is the region most susceptible to S1 nuclease in both tRNAs. The lesser susceptibilities to S1 digestion of the D and TΨC loops in both tRNAs suggest that in solution these molecules have tertiary interactions consistent with the known crystal structure of yeast tRNA^{Phe}. S1 mapping of an end-labeled 40 nucleotide fragment of *E. coli* tRNA$^{Glu}_2$ generates a pattern of oligonucleotides consistent with the cloverleaf structure of the intact tRNA. This result demonstrates that the method is capable of mapping local secondary structure in detail when tertiary interactions are eliminated.

A variety of physical and chemical techniques can be used to study RNA structure in solution (Bloomfield et al., 1974). With the exception of resonance spectroscopy (T'so et al., 1975; Baan et al., 1977), which is not yet fully developed and requires large amounts of highly purified material, most of these methods provide general structural information regarding the extent and nucleotide composition of helical and single-stranded regions. They are unable to pinpoint helical regions and their lengths within a sequence. Conformational change induced by alteration of the physical and chemical environment of RNA in solution can be detected but not described in detail using these traditional approaches. In order to advance the understanding of the role of RNA structure in a wide range of biological processes, empirically derived, detailed descriptions of the structure of RNA in aqueous solution are needed.

This paper presents a general method for mapping the structure of RNA in solution using an enzyme as probe. The method has the potential to determine the exact locations of paired and unpaired bases in the sequences and to detect conformational transitions induced by changes in the physical state of the solution.

Figure 1 is a flow diagram which summarizes the structure mapping technique. The approach is designed after the DNA sequencing method of Maxam & Gilbert (1977). Data are presented in this paper that demonstrate its feasibility using yeast tRNA^{Phe} and *E. coli* tRNA$^{Glu}_2$, the sequences of which are known (Ohashi et al., 1972; RajBhandary & Chang, 1968).

S1 nuclease, isolated from *Aspergillus oryzae,* can be used to locate single-stranded regions in RNA (Rushizky et al., 1975; Khan & Maden, 1976; Vournakis et al., 1976; Flashner & Vournakis, 1977) and has been shown by Harada & Dahlberg (1975) and others (Rushizky & Mozejko, 1977) to hydrolyze tRNAs primarily in their anticodon loops. This enzyme is used here to probe the structure of 5′-^{32}P-labeled full-length tRNAs and a fragment of *E. coli* tRNA$^{Glu}_2$. Following end labeling and purification by electrophoresis, tRNAs are digested with S1 nuclease so as to cleave fewer than 3% of the labeled molecules in solution. Partial hydrolyses with alkali and base-specific ribonucleases T1, U2, A, and Phy I in urea (Donis-Keller et al., 1977; Simoncsits et al., 1977) are performed in parallel with S1 nuclease reactions without denaturant, and all products are electrophoresed in a 20% polyacrylamide–7 M urea gel. Following autoradiography nucleotides at which tRNA is susceptible to S1 cleavage are located by comparing mobilities of S1-generated bands with those produced by the base-specific nucleases and alkaline hydrolyses. The band patterns obtained contain detailed information consistent with the known three-dimensional structure of tRNA^{Phe} (Jack et al., 1976; Quigley & Rich, 1976) and with the predicted cloverleaf secondary structure of tRNA$^{Glu}_2$ (Ohashi et al., 1974), suggesting that the S1 structure mapping technique can provide reliable structural information for any RNA.

Experimental Procedure

Materials. Brewer's yeast tRNA^{Phe} and *E. coli* tRNA$^{Glu}_2$ were purchased from Boehringer-Mannheim. Baker's yeast unfractionated tRNA (Schwarz/Mann) was deproteinized by phenol extraction. Calf intestinal alkaline phosphatase (Boehringer-Mannheim) was rendered nuclease-free as described (Efstratiadis et al., 1977b) and assayed on *p*-nitrophenyl phosphate (Garen & Levinthal, 1960). T4 polynucleotide kinase was prepared by the method of Panet et al. (1973) or was obtained from New England BioLabs (lot 9). Ribonu-

† From the Department of Biology, Syracuse University, Syracuse, New York 13210. *Received March 6, 1978.* Supported by National Institutes of Health Grant (GM 22280) to J.N.V. and a grant from the Alton-Jones Foundation to the Department of Biology, Syracuse University. A preliminary account of this work has been given (Wurst & Vournakis, 1977).

‡ Department of Biochemistry and Molecular Biology, Harvard University, Cambridge, Massachusetts 02138.

0006-2960/78/0417-4493$01.00/0

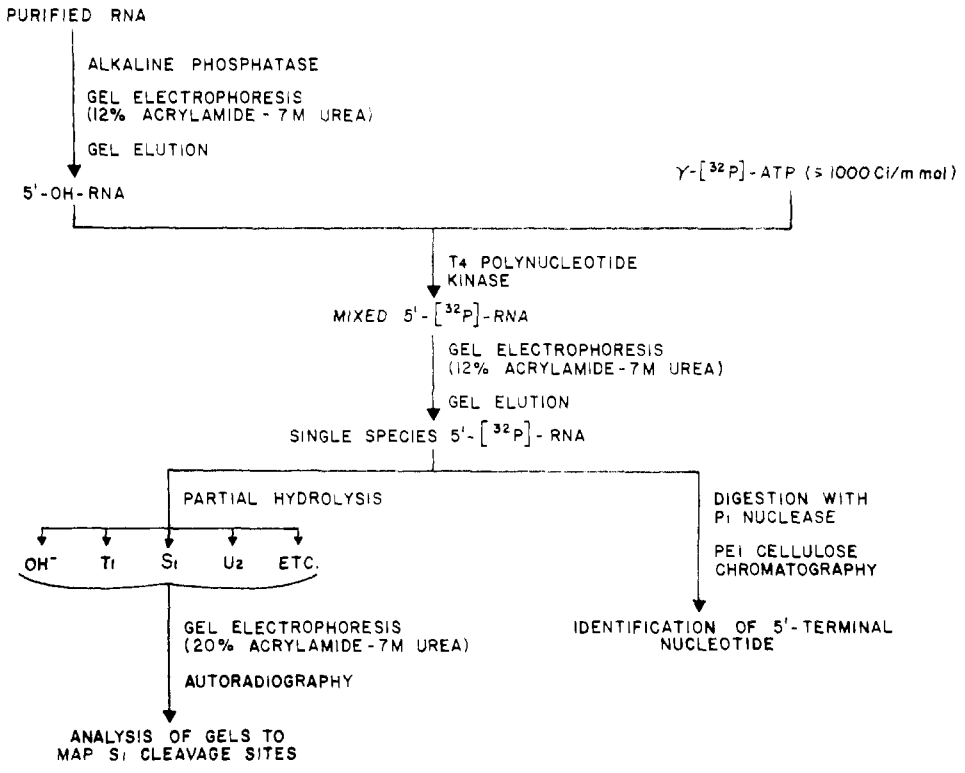

FIGURE 1: Outline of the method used to map structure in RNA.

cleases T1 (Sankyo), U2 (R-Plus, Inc.), P1 (P-L Biochemicals, Inc.) and A (pancreatic) (Worthington) were used without further purification. Phy I nuclease was prepared by the method of Pilly et al. (1978). Polyethyleniminecellulose thin-layer chromatography sheets (Macherey-Nagel) were obtained from Brinkmann Instruments. Acrylamide was from Bio-Rad, and UltraPure urea was from R-Plus, Inc. Reactions were executed in 1.5-mL polypropylene tubes which were siliconized with a 5% (v/v) solution of dichlorodimethylsilane in chloroform. Kodak X-Omat R(XR-5) films and Du Pont Lightning-Plus Intensifying Screens were used for autoradiography. All solutions were prepared using distilled, deionized, autoclaved H_2O. Reaction vessels, capillary pipets, and buffer solutions were autoclaved.

Purification of S1 Nuclease. S1 nuclease was purified from crude α-amylase powder (Sigma Chemicals) by the method of Rushizky et al. (1975), with minor modifications including that the DEAE-cellulose chromatography step was repeated after the CM-cellulose chromatography. The enzyme was found to be free of contaminating RNase T1 and T2 activities. Single-strand specificity of the S1 nuclease preparation at several salt concentrations was confirmed using [^{3}H]poly(rU) and [^{3}H]poly(rA) (Vournakis et al., 1976; Flashner & Vournakis, 1977). Activity of the S1 enzyme was determined by the assay of Vogt (1973).

Dephosphorylation of $tRNA^{Phe}$ and $tRNA^{Glu}_2$. Four nanomoles of tRNA was incubated in 45 μL of 50 mM Tris-HCl (pH 8.3) with 0.045 unit of calf intestinal alkaline phosphatase at 70 °C for 30 min. The reaction mixture was extracted twice with phenol:*m*-cresol 7:1 (v/v) and three times with diethyl ether. The aqueous phase was placed under vacuum, adjusted to 0.2 M in NaAc (pH 5.0), and precipitated with 4 volumes of 95% ethanol by immersion in an ethanol–dry ice bath (−70 °C) for 10 min. The pellet was collected by centrifugation at 12 000*g* for 5 min (Eppendorf microcentrifuge) and was rinsed with 1 mL of 95% ethanol. Following removal of residual ethanol under vacuum, the pellet was redissolved in 25 μL of H_2O. An equal volume of *loading buffer* (0.05% bromophenol blue, 0.05% xylene cyanol, 10 M urea, 40 mM Na_2EDTA) was added, and the mixture was heated at 50 °C for 3 min. The solution was loaded immediately onto a 12% polyacrylamide–7 M urea slab gel (20 cm × 20 cm × 0.3 cm) polymerized from 12% (w/v) acrylamide, 0.4% (w/v) bisacrylamide, 7 M urea, 50 mM Tris–borate (pH 8.3), 1 mM Na_2EDTA. Reservoir buffer was 60 mM Tris–borate (pH 8.3), 1 mM Na_2EDTA. Electrophoresis was conducted at 400 V until the xylene cyanol had migrated 12 cm. The RNA bands were visualized with ultraviolet light (Hassur & Whitlock, 1974). Full-length tRNA was eluted from crushed gel slices into 1 mL of *elution buffer* (0.5 M NH_4Ac, 0.01 M $Mg(Ac)_2$), 0.1 mM Na_2EDTA, 0.1% $NaDodSO_4$)[1] by shaking at 37 °C for 12 h. The eluate was passed through a plastic syringe with a 3-mm siliconized glass wool plug and a 26 G needle. RNA was precipitated in ethanol and recovered by centrifuging at 18 000*g* for 90 min at 5 °C. It was resuspended in 200 μL of 0.2 M NaAc (pH 5.0), reprecipitated in ethanol and sedimented at 12 000*g* for 5 min. The pellet was rinsed with 1 mL of ethanol, centrifuged, and dried as described. Dephosphorylated RNA was dissolved in H_2O and quantitated by determination of absorbance at 260 nm, using an extinction coefficient of 86.6 L cm^{-1} mol^{-1} (tRNA). It was stored in H_2O at −20 °C prior to end labeling.

[γ-^{32}P]ATP Synthesis. [γ-^{32}P]ATP was synthesized (Maxam & Gilbert, 1977) with a specific activity of 1300 Ci/mmol and dried under vacuum immediately before use.

5'-End Labeling. Phosphorylation of 20 pmol of dephos-

[1] Abbreviation used: $NaDodSO_4$, sodium dodecyl sulfate.

phorylated tRNA was accomplished in 5 μL of 10 mM $MgCl_2$, 15 mM β-mercaptoethanol, 50 mM Tris-HCl (pH 8.3) containing 300 pmol of [γ-^{32}P]ATP and 0.45 unit of polynucleotide kinase. The reaction mixture was incubated at 37 °C for 30 min, combined with 20 μL of *loading buffer* heated at 50 °C for 3 min, and electrophoresed as previously noted. Labeled tRNA was located by autoradiography and recovered as described above, except that carrier RNA was added to a concentration of 40 μg/mL before the addition of ethanol. End-labeled tRNA was precipitated with the appropriate isoaccepting tRNA as carrier, while unfractionated tRNA was used to coprecipitate the $tRNA^{Glu}_2$ fragment molecule.

5′-End Analysis. End-labeled RNA was digested exhaustively with P1 nuclease (Lockard & RajBhandary, 1976). Digests were spotted on polyethyleniminecellulose thin-layer sheets and chromatographed in parallel with unlabeled nucleoside 5′-monophosphate markers in 1.0 M LiCl. Standards were visualized with ultraviolet light and marked with ^{32}P-labeled ink. The chromatogram was autoradiographed, and counts were quantitated.

Partial Digestions with Base-Specific Enzymes. The method by which partial digests were achieved in urea has been described elsewhere (Donis-Keller et al., 1977). Ribonuclease T1 at 2×10^{-3} unit/μg of RNA and ribonuclease U2 at 10^{-2} unit/μg of RNA produced suitable partial digests for all substrates. Pancreatic ribonuclease generated partial digests at 9×10^{-5} unit/μg. The activity of the Phy I preparation had not been determined. Appropriate enzyme-to-substrate ratios were obtainable by serial dilutions of the enzyme. Samples for successive loadings were digested simultaneously and stored at −20 °C.

Limited Alkaline Hydrolysis. [^{32}P]RNA was partially hydrolyzed in 10 μL of 50 mM $NaHCO_3/Na_2CO_3$ (pH 9.2), 1 mM Na_2EDTA containing 2.5 μg of unfractionated tRNA carrier by heating at 90 °C for 7 min. An equal volume of *dyes and urea solution* (0.05% bromophenol blue, 0.05% xylene cyanol, 10 M urea) was then added, and samples were loaded onto the gel immediately or stored at −20 °C.

Limited Digestion with S1 Nuclease. In a 10-μL volume [^{32}P]RNA and 10 μg of tRNA were incubated for 1 or 10 min at 37 °C in S1 reaction buffer, 40 mM NaAc (pH 4.5), 0.2 M NaCl, 10 mM $ZnSO_4$, containing S1 nuclease between 6×10^{-2} unit/μg of RNA as specified in the figure legends. Reactions were terminated by adding 1 μL of 0.1 M Na_2EDTA, 1 μL of 10 μg/μL unfractionated tRNA, and 12 μL of *dyes and urea solution.* Samples were kept at −20 °C until electrophoresis.

Gel Electrophoresis. Partial digests were electrophoresed on 20% polyacrylamide–7 M urea slab gels and autoradiographed as described (Donis-Keller et al., 1977; Maxam & Gilbert, 1977). Identical portions of digests were electrophoresed, in some cases, for different times in adjacent lanes. Sequential loadings were made when the xylene cyanol marker of the sample initially loaded had migrated 35 cm from the origin, and electrophoresis was terminated when the bromophenol blue in the final sample had migrated 21 cm.

Results

Preparation of [5′-^{32}P]tRNA. Dehosphorylation of tRNA was optimized with respect to ionic strength, enzyme-to-substrate ratio, and incubation time and temperature. Under the best conditions dephosphorylation is quantitative as determined by the amount of radioactivity released from 5′-^{32}P-end-labeled tRNA tracer. Electropherograms of dephosphorylated tRNAs reveal by UV shadowing a full-length species with minor degradation products. Recovery of full-length dephosphorylated tRNA after electrophoresis, elution, and precipitation is better than 90% based on absorbance measurements. Conditions for the kinase reaction were chosen on the basis of control experiments in which temperature, enzyme-to-substrate ratio, and the concentrations of $MgCl_2$, β-mercaptoethanol, and [γ-^{32}P]ATP were varied. These conditions, which are similar to those recommended by Lillenhaug & Kleppe (1977), result in the labeling of full-length tRNA to a specific activity of at least 15 Ci/mmol routinely. Figure 2A shows that most of the incorporated radioactivity resides in full-length $tRNA^{Phe}$, and that two labeled species, full-length material

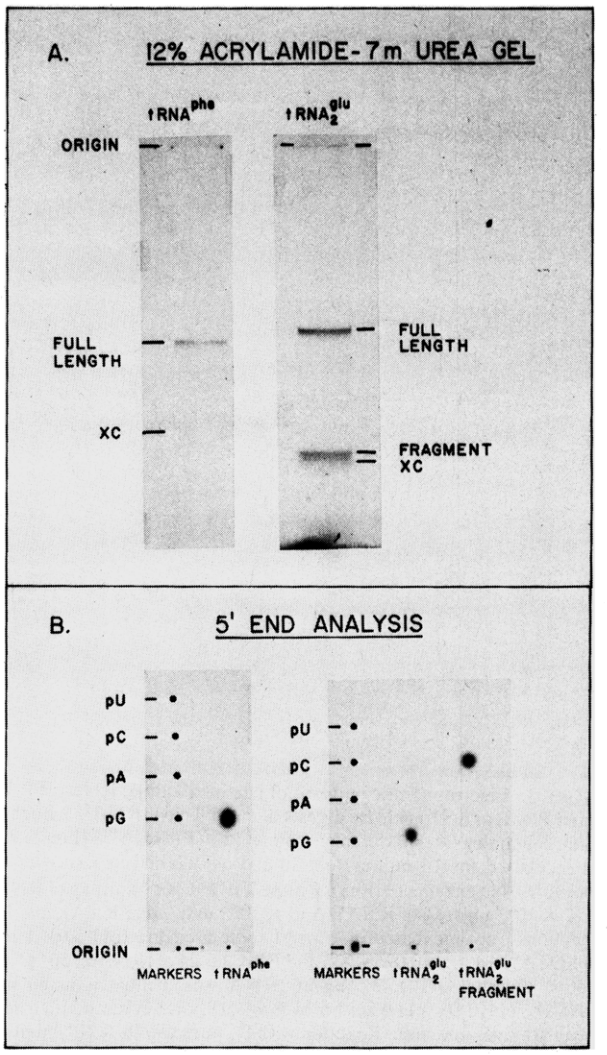

FIGURE 2: Purification and end-group analysis of 5′-^{32}P-end-labeled tRNAs. (A) Autoradiograph of [5′-^{32}P]$tRNA^{Phe}$ and [5′-^{32}P]$tRNA^{Glu}_2$ and fragments of the latter after electrophoresis on a slab gel. Each tRNA was dephosphorylated with alakaline phosphatase, rephosphorylated with polynucleotide kinase and [γ-^{32}P]ATP (1300 Ci/mmol), electrophoresed at 400 V in a 12% polyacrylamide, 7 M urea, 50 mM Tris–borate (pH 8.3), 1 mM Na_2EDTA slab gel until the xylene cyanol (XC) marker had migrated 12 cm and the gel was exposed to Kodak XR-5 film for 1 min, all as detailed under Experimental Procedures. Regions labeled "full-length" and "fragment" were excised from the gel and the labeled RNA eluted and analyzed for end group (Figure 2B) and nucleotide sequence and structures (Figures 3–5). A second $tRNA^{Glu}_2$ fragment migrating slightly faster than "fragment" was not extracted from the gel. (B) Autoradiographs of labeled terminal nucleotides of [5′-^{32}P]$tRNA^{Phe}$, [5′-^{32}P]-$tRNA^{Glu}_2$, and a [5′-^{32}P]$tRNA^{Glu}_2$ fragment after thin-layer chromatography; 0.2% of each end-labeled RNA extracted from the gel of A was digested to mononucleotides with P1 nuclease, and 2 μL of the digests spotted next to unlabeled nucleoside 5′-monophosphates on PEI-cellulose sheets. After chromatography in 1 M LiCl, the marker nucleotides were visualized under UV light, marked with ^{32}P-labeled ink, and autoradiographs of the plates prepared with Kodak XR-5 film.

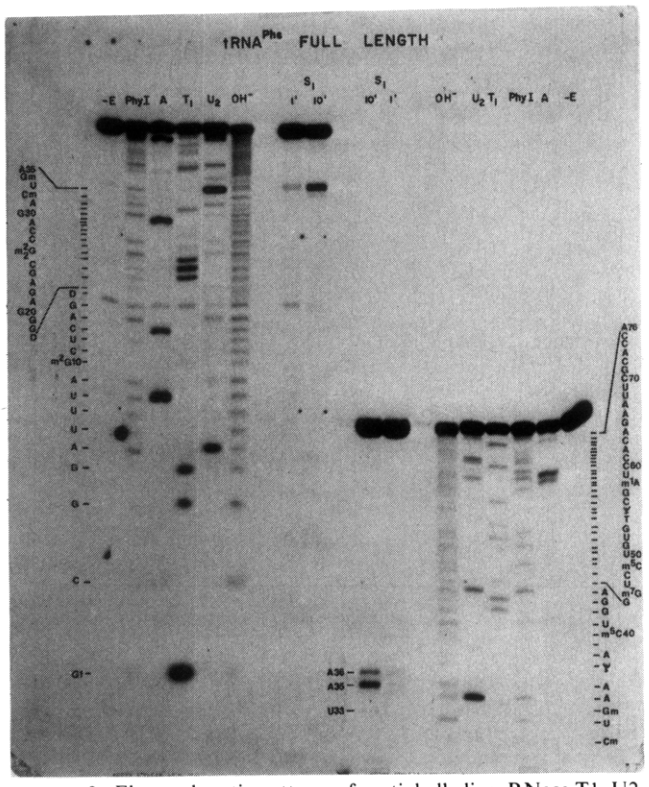

FIGURE 3: Electrophoretic patterns of partial alkaline, RNase T1, U2, A, and Phy I, and S1 nuclease digests of end-labeled $tRNA^{Phe}$. Each reaction, containing 20 000 Cerenkov cpm of [5′-^{32}P]$tRNA^{Phe}$ (Figure 2A), was incubated for 15 min as follows and as detailed in Experimental Procedures. No enzyme (− Enz), RNase T1 (2×10^{-3} unit/μg of RNA), U2 (2×10^{-2} unit/μg of RNA), A (9×10^{-5} unit/μg of RNA), and Phy I reactions were incubated in 20 mM sodium citrate (pH 5.0), 1 mM Na_2EDTA, 7 M urea, 0.025% XC and BPB, 2.5 μg of tRNA at 50 °C. For alkaline digests (OH^-), 2.5 μg of tRNA was incubated in 50 mM $NaHCO_3/Na_2CO_3$ (pH 9.2), 1 mM Na_2EDTA at 90 °C and then combined with dyes and urea. Reaction with S1 nuclease (6×10^{-3} unit/μg of RNA) proceeded in 10 μL of 40 mM NaAc (pH 4.5), 0.2 M NaCl, 10 mM $ZnSO_4$ at 37 °C and was stopped by adding 10 μg of tRNA, 100 nmol of Na_2EDTA, and dyes and urea. Portions of each digest were loaded on 20% polyacrylamide–7 M urea slab gels at intervals and electrophoresed at 1000 V (regulated voltage) to resolve oligomers of different lengths. Electrophoresis was terminated when xylene cyanol (XC) of initial samples moved the equivalent of 50 cm, and BPB of the final loading moved 21 cm. Numbers on diagrams note positions of nucleotides relative to the 5′ end of $tRNA^{Phe}$ as determined with partial sequence data in OH^- (each residue), T1 (G), U2 (A), A (C + U), and Phy (A, G, U) lanes. These data identify sites cleaved by S1 nuclease in reactions electrophoresed in parallel as depicted in Figure 7A.

and a specific fragment molecule, predominate among the products of the kinase reaction involving $tRNA^{Glu}_2$. Recovery of labeled tRNA through elution and precipitation is quantitative as determined by Cerenkov counting. Degradation of the end-labeled product is minimized by storage in 80% ethanol at −20 °C.

5′-End Analysis. The 5′-end analysis, shown in Figure 2B and quantitated by liquid scintillation counting, reveals that more than 98% of the radioactive molecules are labeled at a single nucleotide and that nucleotide is pG as expected for both full-length tRNAs, and pC for the $tRNA^{Glu}_2$ fragment molecule.

Partial Digestions of [5′-^{32}P]$tRNA^{Phe}$ with Alkali and Base-Specific Ribonucleases. Partial alkaline hydrolysis of $tRNA^{Phe}$ generates a sequential array of oligomers as seen in Figure 3. Oligonucleotide lengths are assigned relative to the 5′ end of the molecule. Double bands generated for each dihydrouridine at positions 16 and 17 are believed to terminate in the cyclic intermediate and β-alanine which can be generated under similar reaction conditions (Magrath & Shaw, 1967). Nucleotides 32 and 34, 2′-*O*-methylcytidylic acid and 2′-*O*-methylguanylic acid, respectively, are not cleaved as alkylation at the 2′ position prevents the formation of the 2′:3′-cyclic phosphate intermediate (Brown & Todd, 1955). The pattern of the alkaline hydrolysate is sufficient to allow the unequivocal assignment of oligonucleotide lengths to bands present in the enzyme digests that were electrophoresed in parallel.

Partial digestion of $tRNA^{Phe}$ in urea with ribonuclease T1 generates oligonucleotides terminating in guanosine 3′-monophosphates. The positions of all guanylic acids can be discerned from Figure 3 with the exception of the modified guanylic acid residues resistant to T1 RNase (McCully & Cantoni, 1961; RajBhandary et al., 1968). Figure 3 shows that ribonuclease U2 cleaves $tRNA^{Phe}$ at all adenylic acid residues but m′A-58. Base methylation of this nucleotide at the N1 position would be expected to inhibit its cleavage (Uchida et al., 1970). The Phy I enzyme is cleaving most purines, all uridylic acids including D16, D17, Ψ39, and ψ55, but no cytidylic acids. Ribonuclease A has hydrolyzed at some pyrimidines throughout $tRNA^{Phe}$. Coordination of these data (Figure 3) allows definition of uridylic and cytidylic acid positions within the $tRNA^{Phe}$ sequence.

Partial Cleavage of [5′-^{32}P]$tRNA^{Phe}$ with S1 Nuclease. Partial cleavage patterns produced by alkali and base-specific ribonucleases allow the assignment of specific oligonucleotide lengths to fragments present in the S1 nuclease digests of end-labeled $tRNA^{Phe}$ electrophoresed simultaneously. Figure 3 demonstrates the ability to resolve S1 cleavage products from the $tRNA^{Phe}$ molecule which differ in length by a single nucleotide. The most striking feature of the S1 digestion patterns is the dramatic intensity with which the enzyme cleaves the anticodon loop. The susceptible residues are nucleotides 33, 35, and 36 (Figure 5). There are sites in the D and TΨC loops that are consistently cleaved by S1 nuclease. These exact positions have yet to be identified unequivocably as they are cleaved with low probabilities and, therefore, generate bands of light intensities on autoradiograms. The most intense cleavages introduced into $tRNA^{Phe}$ by S1 nuclease are positioned on the cloverleaf model in Figure 7A.

Partial Digestions of [5′-^{32}P]$tRNA^{Glu}_2$. Partial digestion patterns of end-labeled $tRNA^{Glu}_2$ with alkali and base-specific nucleases are displayed in Figure 4 (see paragraph concerning supplementary at the end of this paper). Ribonucleases T1 and U2 generate all expected fragments terminating in guanylate or adenylate residues, respectively. Positions and identities of the pyrimidines are ascertained by patterns in the Phy I and RNase A lanes. Sites cleaved by S1 under native conditions could be mapped within the $tRNA^{Glu}_2$ sequence when correlated with the alkali and base-specific ribonuclease bands. Residues consistently susceptible to cleavage by S1 nuclease are at positions 20, 34, 35, 36, and 37 (Figure 4). The most intense bands obtained by S1 digestion of $tRNA^{Glu}_2$ arise from cleavages in the anticodon loop at nucleotides 34, 35, 36, and 37; therefore, the anticodon loop is again the most accessible region in the tRNA for S1 nuclease (Figure 5). The S1 nuclease susceptibility map for $tRNA^{Glu}_2$ is presented on a cloverleaf framework in Figure 7B.

Partial Digestion of the [5′-^{32}P]$tRNA^{Glu}_2$ Fragment Molecule. Figure 6 presents the results of coordinated sequence and structure mapping of one end-labeled $tRNA^{Glu}_2$ fragment isolated from among several after reaction of full-length tRNA with polynucleotide kinase and [γ-^{32}P]ATP (Figure 2A). When the fragment is partially digested with RNases T1, U2, and A, the following partial sequence is obtained, in which Y

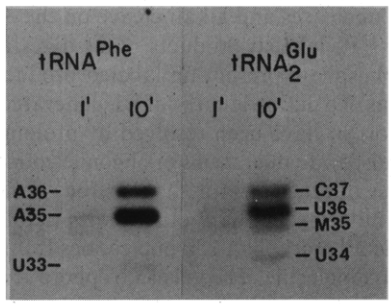

FIGURE 5: S1 cleavages in the anticodon loop of $tRNA^{Phe}$ and $tRNA^{Glu}_2$. Comparison of 1′ and 10′ digestion patterns in the anticodon loop regions of the two tRNAs is made. Reaction conditions are identical with those described in Figures 3 and 4.

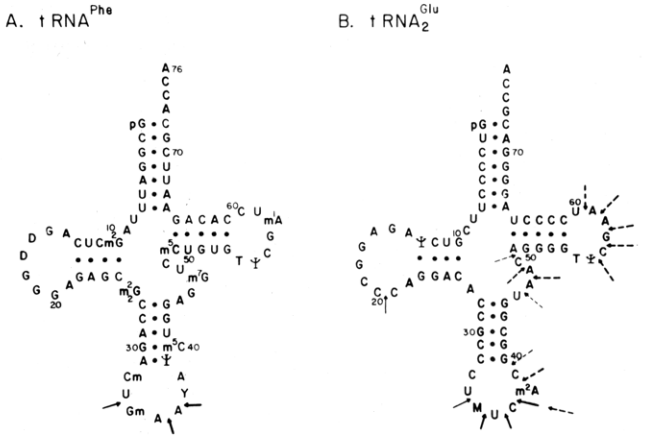

FIGURE 7: Cloverleaf models of (A) yeast $tRNA^{Phe}$ and (B) *E. coli* $tRNA_2^{Glu}$ showing the susceptibilities of nucleotides to digestion by S1 nuclease. Heavy arrows denote regions more susceptible to hydrolysis by S1, and thin arrows indicate sites cleaved by S1 to a lesser extent. (A) Solid lines mark positions dramatically cleaved upon S1 treatment. (B) Solid arrows mark sites of the full-length [5′-^{32}P]$tRNA_2^{Glu}$ which are hydrolyzed. All dotted arrows represent S1 cleavages introduced into the 40 nucleotide fragment molecule of $tRNA_2^{Glu}$ in the presence of unfractionated tRNA carrier.

represents a pyrimidine and X represents an unidentified nucleotide:

5′-[^{32}P]CXYGGYGGYAAYXGGGGXXYGAAYXXX-YXAGGGG . . .

This sequence identifies the 5′-terminal nucleotide as the cytidylic acid at position 37 in the anticodon loop; this is consistent with the end analysis of Figure 2B. Figure 4 indicates that position 36 is the site most susceptible to S1 nuclease in full-length $tRNA^{Glu}_2$, and the cleavage which generates the fragment is at this same site. This fragment affords the opportunity to study structure in the 3′ half of $tRNA^{Glu}_2$ presumably in the absence of most tertiary interactions. S1 nuclease patterns from this fragment molecule demonstrate, for example, cleavage at every nucleotide in the extra loop while nucleotides 44 and 49 on either side of this loop are untouched. At all three enzyme-to-substrate ratios used S1 nuclease generates an identical pattern of cleavages at positions 38, 39, 45–48 (variable loop), and 54–58 (TΨC loop). Even in cases of overdigestion S1 nuclease fails to generate mononucleotides under conditions used here (unpublished data). This observation is consistent with the absence of a band corresponding to nucleotide 37 which presumably is not hydrogen bonded. Less intense breaks are introduced near the 3′ end of the fragment, but exact nucleotide lengths cannot be assigned. Regions in the fragment corresponding to G:C rich acceptor and anticodon stems are not cleaved by S1 nuclease (Figure 7B). Thus, the 3′ end of the molecule maps as a partial cloverleaf with both the variable loop and the TΨC loops single stranded.

Discussion

The RNA structure mapping approach described above has the potential for generating detailed information concerning the locations of hairpin single-stranded loop and helical stem regions in 5′-^{32}P-labeled RNA molecules. End-labeling tRNA with polynucleotide kinase and [γ-^{32}P]ATP (Hanggi et al., 1970; Lillenhaug & Kleppe, 1977; Silberklang et al., 1977), partial enzymatic cleavage using base-specific (Schmidt et al., 1970; Samuelson & Keller, 1972; Streeck & Zachau, 1972; Vigne & Jordan, 1977), or structure-specific (Harada & Dahlberg, 1975; Tal, 1975; Flashner & Vournakis, 1977; Rushizky & Mozejko, 1977) endoribonucleases, and the analysis of tRNA fragment molecules (Zachau et al., 1974), are combined with high resolution polyacrylamide gel electrophoresis to produce a rapid technique for mapping structure in molecules whose primary sequences are known.

Digestion of end-labeled tRNA with S1 nuclease generates oligonucleotide fragments of discrete lengths. The data presented in this paper demonstrate that full-length $tRNA^{Phe}$ and $tRNA^{Glu}_2$ have limited susceptibilties to S1 digestion, as expected (Harada & Dahlberg, 1975; Rushizky & Mozejko, 1977). The S1 nuclease, under conditions designed to generate partial digestion and structural information, attacks these molecules in their loops, with particular preference for the anticodon loops. S1 nuclease also hydrolyzes, though a limited extent, at particular sites in the D and TΨC loops in these molecules. The relative susceptibilities of different cleavage sites can be judged qualitatively by comparing intensities of bands on the autoradiograms. It is seen in Figures 3 and 7A that cleavage of $tRNA^{Phe}$ in the anticodon loop is much more probable than in the D and TΨC loops. The S1 digestion patterns of $tRNA^{Phe}$ are consistent with its known secondary and tertiary structure (Jack et al., 1976; Quigley & Rich, 1976). No digestion is observed at bases that exist within helices. In $tRNA^{Phe}$ crystals the anticodon loop is the most protruding region, whereas the D and TΨC loops, known to interact via hydrogen bonds, would be less available for cleavage. The results with $tRNA^{Glu}_2$ are similar (Figures 4 and 7B). The similarity of the patterns of S1 nuclease digestion of the two tRNAs is consistent with the expectation that all tRNAs may assume similar tertiary structures in solution (Kim, 1976).

The remarkable results with the forty nucleotide fragment of $tRNA^{Glu}_2$ shown in Figures 6 (supplementary material) and 7B demonstrate that secondary structure can be mapped directly and in detail provided that tertiary interactions have been disrupted. In this case fortuitous specific cleavage of the full-length $tRNA^{Glu}_2$ in the anticodon and end labeling at the cleavage site occurred. The gel of Figure 2A seems to have resolved the 40 nucleotide labeled fragment from the 36 nucleotide unlabeled portion of the intact molecule. Hence, nucleotides in the variable and tΨC loops cannot form tertiary interactions, and they become accessible to S1 nuclease. The protection of anticodon stem and acceptor stem nucleotides from cleavage by S1 nuclease was unexpected as half of these stems are missing in the labeled fragment. Electropherograms of unfractionated tRNA carrier used in the Figure 6 experiment reveal the presence of short oligonucleotides. It was hypothesized that these fragments in the carrier tRNA, present during S1 nuclease reactions, could hybridize to the G:C rich ends of the $tRNA^{Glu}_2$ fragment and afford them protection

from S1 hydrolysis. S1 nuclease digestions of the [5′-^{32}P]-$tRNA^{Glu}_2$ fragment were repeated either without carrier or with purified full-length tRNA, *E. coli* 5S rRNA, or poly(A)·poly(U) as carrier substrates. The TΨC stem remained resistant to digestion in all cases while both the anticodon and acceptor stems were cleaved by S1 nuclease although to a lesser extent than this hypothesis would predict (data not shown).

There seem to be discrepancies between the data presented here for S1 nuclease and the expected susceptibilities of particular nucleotides in yeast $tRNA^{Phe}$ to attack by nucleases. The crystal model for $tRNA^{Phe}$ predicts that nucleotides D16, D17, G20, U47, G57, and U59 ought to be accessible to S1 nuclease digestion as these bases are not hydrogen bonded. Weak autoradiographic bands are consistently found that may represent these cleavages, but digestion seems minimal. For example, G20 in the D loop is not substantially cleaved by S1 nuclease, whereas it is hydrolyzed upon partial digestion with RNase T1 under different experimental conditions (Schmidt et al., 1970; Samuelson & Keller, 1972; Rich & RajBhandary, 1976). Although G20 has not been implicated in tertiary interactions, both G19 and A21 are hydrogen bonded to C56 and m^7G46, respectively, in the crystal model (Jack et al., 1976; Quigley & Rich, 1976). As Dodgson & Wells (1977) have reported that single base mismatches within DNA are extremely resistant to S1 nuclease, the enzyme may have a similar substrate specificity for RNA. Thus, the inaccessibility of G20 to S1 nuclease might be expected. Its mass may prevent the larger S1 nuclease (mol wt 32 000) (Vogt, 1973) from cleaving $tRNA^{Phe}$ at G20, a position readily available to RNase T1 (mol wt 11 000) (Egami et al., 1964). Under the conditions of the S1 reaction it is possible, too, that local folding of the backbone may prevent nucleolytic attack of G20. Similar arguments may be invoked to rationalize the inavailability of U47 and G57 to S1 nuclease. Neither residue is hydrogen bonded, and each is positioned between two nucleotides that participate in tertiary interactions (Jack et al., 1976; Quigley & Rich, 1976). The U47 and G57 may fail to satisfy the minimal substrate dimensions for S1 nuclease. These nucleotides might be protected from hydrolysis due to local backbone folding (U47) or stacking within the interior of $tRNA^{Phe}$ (G57). The minimal substrate dimensions requisite for S1 nuclease activity (Dodgson & Wells, 1977) may explain the failure of the enzyme to hydrolyze non-hydrogen-bonded bases adjacent to hairpin helices. Modified bases, for example, Cm32, Gm34, and Y37 in the anticodon, appear to be poorer substrates for S1 nuclease then their unmodified analogs.

The structure map of $tRNA^{Phe}$ generated by S1 nuclease bears close resemblance to that known to exist in crystals. Refinement of the method presented here, though, is required before it can be applied confidently to molecules for which the rigorous criterion of a crystallographic model does not exist.

There are limitations with the RNA structure mapping technique. One problem is in rigorous identification of those nucleotides susceptible to the structure specific nuclease. It is crucial to obtain definitive sequence information in each structure mapping experiment and is, therefore, important to display in parallel as many base-specific sequence patterns as possible. It is also necessary, particularly for work with the tRNAs, to define both susceptibilities of modified bases to alkali and all nucleases used, and the electrophoretic behavior of such products. Correct assignment of S1 cleavage sites close to the labeled end requires that one be aware of the different mobilities of S1-generated fragments and those of the same lengths produced by the base-specific ribonucleases. S1 nuclease cleaves on the 5′ side of phosphodiester bonds, while the base-specific nucleases and alkali cleave on the 3′ side. Consequently, 5′-^{32}P]-labeled products of S1 digestion lack the 3′-terminal phosphate present on labeled products from the other reactions. To define lengths of S1-generated fragments which are short or have been resolved by prolonged electrophoresis, the disparate migrations of oligonucleotides produced by S1 nuclease of other treatments must be considered.

Another limitation of the method is its inability to map structure in detail more than 150 nucleotides from the labeled end of an RNA molecule. The gel electrophoretic system does not resolve single nucleotide differences in polynucleotides with chain lengths longer than this. Assignment of S1 cleavage sites which are increasingly distant from the labeled terminus can be facilitated by loading portions of samples at several times during electrophoresis so that longer oligonucleotides are eventually resolved. Labeling of a unique RNA 3′ end and digestion with the structure-specific enzyme can yield a detailed structure map for the 150 nucleotides proximal to the 3′ end of a molecule.

At its current level of development the structure mapping method described can identify individual nucleotides of an RNA molecule which are not hydrogen bonded in solution. The data presented for both full-length tRNAs, though consistent with the crystallographic model of $tRNA^{Phe}$, are yet incomplete. All non-hydrogen-bonded bases in $tRNA^{Phe}$, for example, are not cleaved by S1 nuclease. Probable causes include: (1) the apparent resistance of the Y-base and the 2′-O-methylated bases in the anticodon loop to S1 nuclease under conditions used here and (2) the apparent requirement for S1 activity of several contiguous non-hydrogen-bonded bases in a substrate. Furthermore, extensive hydrogen bonding among the D, variable, and TΨC loops prevents the complete exposition of structure in each independent loop. The structure mapping method is being extended to probe for non-hydrogen-bonded bases under less restrictive solution conditions at high temperatures and pH with less salt.

The comprehensive elucidation of tRNA structure in solution must include information on the relative susceptibilities of non-hydrogen-bonded nucleotides to the structural probe, here, S1 nuclease. These data are becoming available through the systematic variation of reaction time and such parameters as are mentioned above. The different patterns present in the S1 lanes of Figure 3, for example, demonstrate the value of the study of $tRNA^{Phe}$ susceptibility to S1 nuclease as a function of time. Cleavages introduced into the anticodon loop within 1 min suggest the extreme accessibilities of nucleotides 35 and 36, whereas position 33, though less accessible to the S1, is hydrolyzed within 10 min. Ultimately such relative susceptibilities can be accurately quantitated through densitometry of autoradiograms.

Once the dynamics of digestion with S1 nuclease are well characterized on a molecule already analyzed crystallographically, $tRNA^{Phe}$, the expanded method ought to prove invaluable in probing the structures of other RNA molecules and RNA:RNA and RNA:protein complexes of physiological importance.

The RNA literature is replete with hypothetical hairpin structures for which functions have been suggested. Examples include the termination of transcription at points just beyond hairpins in nascent mRNAs (Korn et al., 1977; Lee & Yanofsky, 1977), the recognition of specific cleavage sites by enzymes such as RNase III involved in processing precursor RNA to mRNA (Robertson et al., 1977; Rosenberg & Kramer, 1977), and the binding of ribosomes to initiate protein synthesis at the 5′-non-coding region of mRNA (Efstratiadis et al., 1977a). This method provides a way to search for these

presumptive structures quickly and under conditions which can be varied in both structural and parallel functional experiments.

Acknowledgments

We thank Dr. G. Pavlakis and L. Rieser for purification of S1 nuclease, H. Donis-Keller for the generous gift of the Phy I enzyme, J. Dick and M. A. Katopes for technical assistance, H. Donis-Keller, G. Quigley, A. Rich, N. Vamvakopoulos, and P. Wrede for helpful discussions, G. Chaconas for a gift of RNase-free alkaline phosphatase, and B. Carns for typing.

Supplementary Material Available

Figure 4 showing gel sequencing and S1 nuclease susceptibility data for $tRNA^{Glu}_2$ and Figure 6 showing partial sequencing and S1 susceptibility data for the fragment of $tRNA^{Glu}_2$ (4 pages). Ordering information is given on any current masthead page.

References

Arima, T., Uchida, T., & Egami, F. (1968) *Biochem. J. 106,* 609.

Bann, R. A., Hilbers, C. W., VanCharldorp, R., VanLeerdom, E., VanKnippenberg, P. H., & Bosch, L. (1977) *Proc. Natl. Acad. Sci. U.S.A. 74,* 1028.

Bloomfield, V. A., Crothers, D. M., & Tinoco, I. (1974) *Physical Chemistry of Nucleic Acids,* Harper & Row, New York, N.Y.

Brown, D. M., & Todd, A. R. (1955) in *The Nucleic Acids* (Chargaff, E., & Davidson, J. N., Eds.) p 409, Academic Press, New York, N.Y.

Dodgson, J. B., & Wells, R. D. (1977) *Biochemistry 16,* 2374.

Donis-Keller, H., Maxam, A. M., & Gilbert, W. (1977) *Nucleic Acids Res. 4,* 2527.

Efstratiadis, A., Kafatos, F. C., & Maniatis, T. (1977a) *Cell 10,* 571.

Efstratiadis, A., Vournakis, J. N., & Donis-Keller, H., Chaconas, G., Dougall, D. K., & Kafatos, F. C. (1977b) *Nucleic Acids Res. 4,* 4165.

Egami, F., Takahashi, K., & Uchida, T. (1964) *Prog. Nucleic Acid Res. Mol. Biol. 3,* 59.

Flashner, M. S., & Vournakis, J. N. (1977) *Nucleic Acids Res. 4,* 2307.

Garen, A., & Levinthal, C. (1960) *Biochim. Biophys. Acta 38,* 470.

Hanggi, U. J., Streeck, R. E., Voigt, H. P., & Zachau, H. G. (1970) *Biochim. Biophys. Acta 217,* 278.

Harada, F., & Dahlberg, J. E. (1975) *Nucleic Acids Res. 2,* 865.

Hassur, S. M., & Whitlock, H. W., Jr. (1974) *Anal. Biochem. 59,* 162.

Horne, J. R., & Erdmann, V. A. (1972) *Mol. Gen. Genet. 119,* 337.

Jack, A., Ladner, J. E., & Klug, A. (1976) *J. Mol. Biol. 108,* 619.

Khan, M. S. N., & Maden, B. E. H. (1976) *FEBS Lett. 72,* 105.

Kim, S. H. (1976) *Prog. Nucleic Acid Res. Mol. Biol. 17,* 181.

Korn, L. J., Queen, C. L., & Wegman, M. N. (1977) *Proc. Natl. Acad. Sci. U.S.A. 74,* 4401.

Lee, F., & Yanofsky, C. (1977) *Proc. Natl. Acad. Sci. U.S.A. 74,* 4365.

Lillehaug, J. R., & Kleppe, K. (1977) *Nucleic Acids Res. 4,* 373.

Lockard, R. E., & RajBhandary, U. L. (1976) *Cell 9,* 747.

Lockard, R. E., Alzner-Deweered, B., Heckman, J. E., MacGee, J., Tabor, M. W., & RajBhandary, U. L. (1978) *Nucleic Acids Res. 5,* 37.

Magrath, D. I., & Shaw, D. C. (1967) *Biochim. Biophys. Res. Commun. 26,* 32.

Maxam, A. M., & Gilbert, W. (1977) *Proc. Natl. Acad. Sci. U.S.A. 74,* 560.

McCully, K. S., & Cantoni, G. L. (1961) *Biochim. Biophys. Acta 51,* 190.

Ohashi, Z., Harada, F., & Nishimura, S. (1974) *FEBS Lett. 20,* 239.

Panet, A., VandeSande, J. H., Loewen, P. C., Khorana, H. G., Raae, A. J., Lillehaug, J. R., & Kleppe, K. (1973) *Biochemistry 21,* 5045.

Pilly, D., Niemeyer, A., Schmidt, M., & Bargetzi, J. P. (1978) *J. Biol. Chem. 253,* 437.

Quigley, G. J., & Rich, A. (1976) *Science 194,* 796.

RajBhandary, U. L., & Chang, S. H. (1968) *J. Biol. Chem. 243,* 598.

RajBhandary, U. L., Stuart, A., & Chang, S. H. (1968) *J. Biol. Chem. 243,* 584.

Rich, A., & RajBhandary, U. L. (1976) *Annu. Rev. Biochem. 45,* 805.

Robertson, H. D., Dickson, E., & Dunn, J. J. (1977) *Proc. Natl. Acad. Sci. U.S.A. 74,* 822.

Rosenberg, M., & Kramer, R. A. (1977) *Proc. Natl. Acad. Sci. U.S.A. 74,* 984.

Rushizky, G. W., & Mozejko, J. H. (1977) *Anal. Biochem. 77,* 562.

Rushizky, G. W., Shaternikov, V. A., Mozejko, J. H., & Sober, H. A. (1975) *Biochemistry 14,* 4221.

Samuelson, G., & Keller, E. B. (1972) *Biochemistry 11,* 30.

Schmidt, J., Buchardt, B., & Reid, B. R. (1970) *J. Biol. Chem. 245,* 5743.

Silberklang, M., Gillum, A. M., & RajBhandary, U. G. (1977) *Nucleic Acids Res. 4,* 4091.

Simoncsits, A., Brownlee, G. G., Brown, R. S., Rubin, J. R., & Guilley, H. (1977) *Nature (London) 269,* 833.

Streeck, R. E., & Zachau, H. G. (1972) *Eur. J. Biochem. 30,* 382.

Tal, J. (1975) *Nucleic Acids Res. 2,* 1973.

T'so, P. O. P., Alderfer, J. L., Borer, P. N., & Kan, L. S. (1975) in *Structure and Conformation of Nucleic Acids and Protein–Nucleic Acid Interactions* (Sundaralingam, M., & Rao, S. T., Eds.) p 193, University Park Press, Baltimore, Md.

Uchida, T., Arima, T., & Egami, F. (1970) *J. Biochem. (Tokyo) 67,* 91.

Vigne, R., & Jordan, B. R. (1977) *J. Mol. Evol. 10,* 77.

Vogt, V. M. (1973) *Eur. J. Biochem. 33,* 192.

Vournakis, J. N., Flashner, M. S., Katopes, M. A., Kitos, G. A., Vamvakopoulos, N. C., Sell, M. S., & Wurst, R. M. (1976) *Prog. Nucleic Acid Res. Mol. Biol. 19,* 233.

Wurst, R. M., & Vournakis, J. N. (1977) *J. Cell Biol. 75,* 356a.

Zachau, H. G., Fittler, F., Harbers, K., Phillippsen, P., Thiebe, R., & Wintermeyer, W. (1974) in *XXIVth International Congress of Pure and Applied Chemistry,* Vol. 2, p 45, Butterworths, London.